Mine Water and the Environment (2021) 40:657–670
https://doi.org/10.1007/s10230-020-00748-w

TECHNICAL ARTICLE

Prediction and Prevention of Water Inrush Hazards from Bed Separation Space

Luyuan Wu[1,2] · Haibo Bai[2] · Dan Ma[3]

Received: 6 September 2019 / Accepted: 16 December 2020 / Published online: 5 January 2021

Abstract

The rock plate (RP) method can be used to identify the size and location of potentially dangerous bed separation space (BSS) in coal mines. The RP method is performed in three steps: (1) The rock strata above the coal seam is simplified as a composite plate calculation model; (2) The deflection of rock strata is expressed as a double trigonometric series and obtained using the energy method; (3) The internal-forces and deformation of the RP are solved to determine the size and location of the BSS based on elasticity and a BSS identification process. This requires that the BSS be unbroken, and the BSS upper rock stratum be an aquifer. In this study, the Yuanzigou coal mine was taken as a study case and the RP method was used to determine the size and location of BSS water (BSS-W) above the coal goaf of working face 1,012,001. BSS usually occurs at the contact surface between hard and soft rock strata; at this mine, BSS-W exists between the Yijun conglomerate and the Anding mudstone formations. The results predicted that when the working face advanced 350 m, the third BSS will break, allowing BSS-W to flood into the goaf. These results were verified by borehole video observation. Therefore, two control methods were used: inclined drainage holes drilled from the roadway and spaced holes drilled from the surface in areas with abundant water. This paper thus provides a way to locate the BSS-W and prevent an inrush hazard.

Keywords Coal mining · Rock plate

Introduction

Bed separation space (BSS) refers to a convex lenticular space formed by dissimilar deformation among the rock strata above the coal seam roof. As the BSS increases in size and accumulates water, the force of the upper hard rock strata and the hydrostatic head pressure can cause the lower BSS rock strata to break, leading to BSS water (BSS-W) flowing into the working face. As a result, a BSS-W inrush hazard (BSS-WIH) occurs, which is like a water inrush in old goaf (Fig. 1). Figure 1 also shows the distribution of coal mines with BSS-WIH in China. BSS-WIH is mainly an issue in coal mines located in southwest Shanxi province and southeast Gansu province. Since BSS-WIH can cause large casualties and property damage (Cao 2018; Gao and Sang 2017; He 2018; Qiao et al. 2014), improving identification and management techniques is critical to ensure safe coal production.

The generation of BSS has received broad attention (Gui et al. 2018; Palchik 2003; Palchik 2005; Wang et al. 2017; Xu 2004; Yan et al. 2016). Qian et al. (2003) proposed that the overburden strata of coal goaf (CG) acted like a composite girder and calculated the deformation of overburden strata based on girder theory; then the location of the key rock strata, which controls the deformation of overburden, was identified. The same approach can be used to accurately identify the location of BSS during mining and obtain the height of the fissure zone. BSS has also been studied by key

Supplementary Information The online version contains supplementary material available at https://doi.org/10.1007/s10230-020-00748-w.

✉ Dan Ma
dan.ma@cumt.edu.cn

Luyuan Wu
TB17220023B0@cumt.edu.cn; wulymp@henu.edu.cn

[1] School of Civil Engineering and Architecture, Henan University, Kaifeng 475001, Henan, China

[2] State Key Laboratory for Geomechanics and Deep Underground Engineering, China University of Mining and Technology, Xuzhou 221116, Jiangsu, China

[3] State Key Laboratory of Coal Resources and Safe Mining, School of Mines, China University of Mining and Technology, Xuzhou 221116, Jiangsu, China

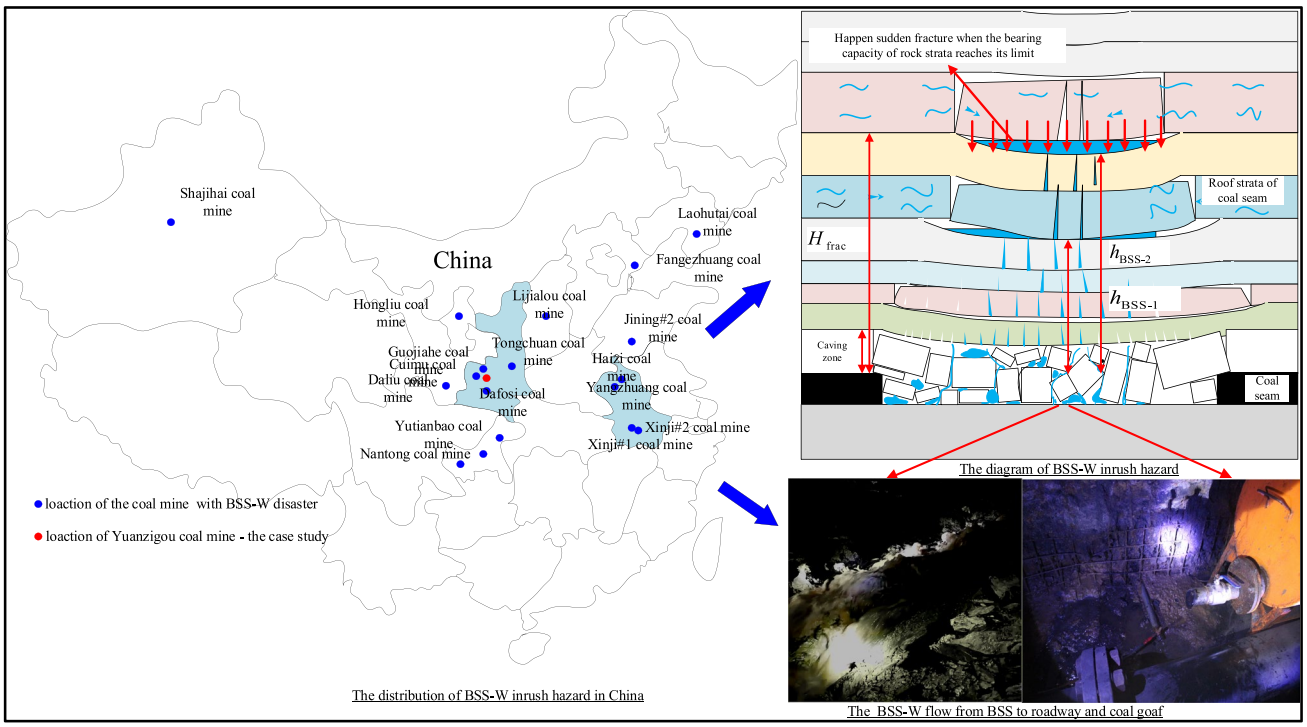

Fig. 1 The distribution of BSS-W inrush hazards in China

strata theory or expanded composition girder theory (Fan et al. 2019; Guo et al. 2016; Li 2011; Miao et al. 2011; Qiao et al. 2014; Xu et al. 2004; Xuan and Xu 2014). However, when the strata above the CG are similar to composite thin plates rather than composite girders, the size and shape of the BSS cannot be obtained in the same manner. Gui et al. (2018) developed the composite rock sheets supposition, an extension of the composite girder method, in which the plate's force mechanism is ignored. He et al. (2018) developed a revised composition rock girder method to locate the BSS, in which the influence of any stratum on the overall deformation of overburden and the interaction between two adjacent strata were considered. However, the shape and size of the BSS could not be obtained, and the real coal mining conditions were rarely considered in the rock girder calculation model, compared with the rock plate calculation model.

Discrete element numerical simulation was also used to identify the BSS (Chen and Guo 2008; He 2018; Li 2011; Qiao et al. 2014; Su et al. 2003; Wu et al 2019). This method simulates the response of jointed rock systems or discontinuous block systems under static or dynamic loads. However, the discrete element method has not been fully developed and lacks mathematical support; most discrete methods adopt an explicit algorithm, which leads to an error transfer problem, and there is no corresponding solution (Ma et al. 2019, 2020a; Zhou et al. 2018).

A field simulation experiment is also a good way to study the development of BSS and the height of the fissure zone (He 2018; Li 2011; Qian et al. 2003). The laboratory model is designed using the principle of similarity; then mechanical parameters and distribution rules of the model are observed with the aid of testing instruments, allowing the possible mechanical behavior and rock stress distribution to be inferred in the prototype (Ma et al. 2021). However, plane simulation experiments are mainly performed without accounting for the horizontal size of the plane model. Also, because boundary conditions of the plane model are greatly simplified, the accuracy of simulation results is greatly reduced.

BSS-W is another necessary condition. BSS-W is derived from the upper rock strata, usually an aquifer with a large permeability coefficient (Cao 2018; He 2018; Qiao et al. 2014). BSS-W accumulates in the BSS until the rock supporting the BSS fractures (Ma et al. 2020b; Qiao et al. 2014). However, the volume of BSS-W and its relationship to water flow has rarely been investigated.

The development of a longitudinal fissure zone into the BSS is the immediate cause of a BSS-WIH. Xu et al. (2009) studied the impact of primary key stratum (PKS) location on the evolution of a water-flowing fracture by simulation experiments and engineering exploration. Lu et al. (2018) assessed the risk of BSS-W inrush using the analytic hierarchy process method. Palchik (2003) considered that the

maximum height of an interconnected fracture zone may reach 19–41 times the thickness of the coal seam, and determined that horizontal fractures may extend 53–92 times the coal seam's thickness. Borehole observation experiments above the CG is the most accurate way to determine the height of such fissure zones (He et al. 2018; Lin and Qiao 2016). However, these methods are highly expensive. To effectively control BSS-W, Qiao et al. (2011, 2014) proposed controlling BSS-W by constructing a diversion hole and a straight ground diversion hole to promote the release of the BSS-W. However, the drilling capacity of the roadway was ignored. In addition, there is a large distance between the aquifer bottom and drive pipe bottom when constructing a straight diversion hole. This leads to water from the aquifer to constantly flow into the CG, leading to expensive pumping requirements and a large waste of water resources. In summary, the above methods should be improved from the following aspects: a calculation model is required that is more consistent with the force conditions of the coal seam roof; the BSS identification theory needs to be more fully studied and verified, and; more control measures are needed to ensure safe production, reduce drainage costs, and protect water resources. To this end, the deformation and internal forces of a coal seam roof were studied using the rock plate (RP) method. In addition, a method to identify BSS-W was developed, and detailed control measures for BSS-W inrush hazards were proposed and successfully implemented.

The RP Method

To obtain the size and location of BSS, the deformation and equilibrium state of the rock strata above the CG should be accurately calculated. This can be done using the RP method, which is based on thin plate theory and elasticity. Generally, the shape of the working face is square or rectangular. Based on the definition of the thin plate and the character of the rock, the strata above the CG can be taken as a composite thin plate to analyze the deformation and internal forces of rock strata as the working face gradually advances. Next, a yield criterion is proposed. The Drucker–Prager criterion is used to assess RP instability. Finally, the state of the RP can be judged. The distribution and size of the BSS can be obtained by summarizing all of the separation results as the working face advances. More detailed information on the RP method can be accessed through the supplemental file.

The BSS-W Inrush Identification Method

The BSS-W Identification Criteria

The formation of BSSW requires unbroken BSS so that water can be stored in this space (Fig. 2). The upper RP of BSS, the source of the BSS-W, must be an aquifer with a sufficient permeability coefficient. As the BSS forms, the water flows from the aquifer into the BSS. As shown in Fig. 2, the red sandstone is an aquifer. In addition, the lower RP of the BSS must be an aquiclude with a small permeability coefficient, to prevent BSS-W loss. As shown

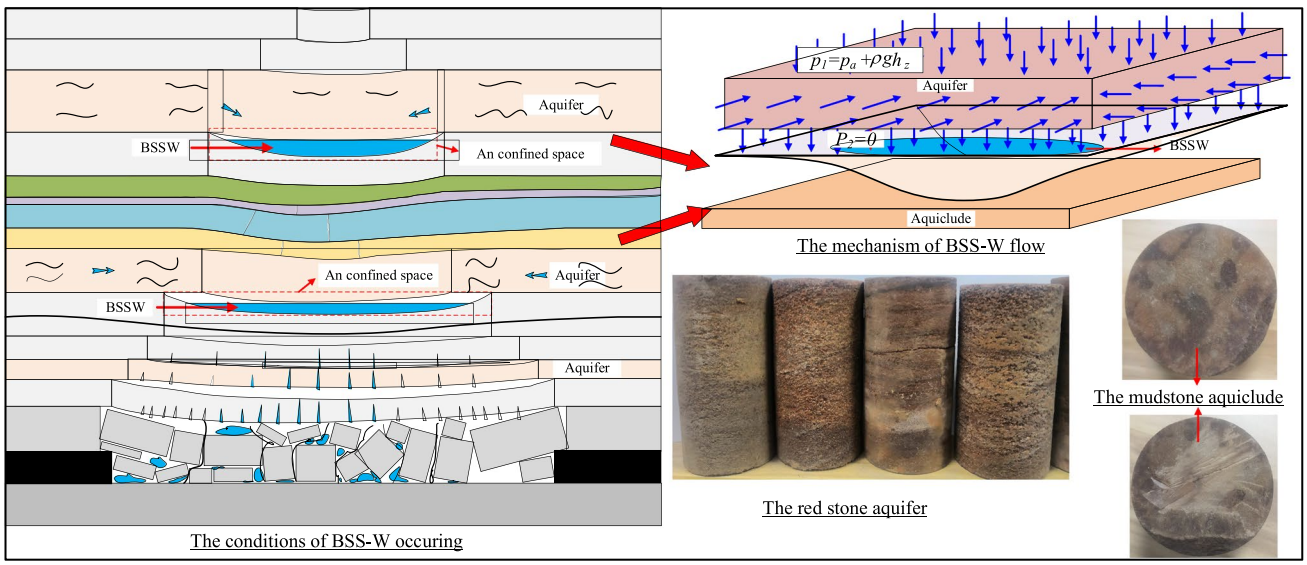

Fig. 2 The formation conditions of BSS-W

in Fig. 2, the mudstone is an aquiclude with a small permeability coefficient.

BSS-W Volume

Figure 2 shows the water flowing from the aquifer into the BSS, in accordance with the one-dimensional flow of Darcy's law. Therefore, water volume Q in BSS is solved by Darcy's law and obtained by Eqs. (1–5).

$$Q = q_w \cdot t_0 = K_i \cdot t_0 \cdot A_i \frac{\Delta p}{\delta_i}, \tag{1}$$

$$Q \le V_{\mathrm{BSS}}, \tag{2}$$

$$A_i = a_i \times b_i, \tag{3}$$

$$\Delta p_0 = p_1 - p_2, \tag{4}$$

$$p_1 = p_a + \rho_w g h_z, \quad p_2 = 0. \tag{5}$$

BSS-W Inrush Criteria

Since the BSS is a confined space, water can continually accumulate there. The volume of the BSS and BSS-W increases with the excavation of the coal seam until the water-conducting fracture zone connects with the BSS, which triggers the BSS-W inrush. The height of the water-conducting fracture zone is a key factor:

a. $H_{\mathrm{frac}} = h_{\mathrm{BSS}-1}$. When the height of water-conducting fracture equals the location of BSS-1, all RPs under the BSS-1 fail and the first BSS-W inrush occurs in the working face.
b. $H_{\mathrm{frac}} = h_{\mathrm{BSS}-2}$. When the height of water-conducting fracture equals the location of BSS-2, all RPs under the BSS-2 fail. The second BSS-W inrush occurs in the working face.
c. $H_{\mathrm{frac}} = h_{\mathrm{BSS}-i}$. When the height of water-conducting fracture equals the location of BSS-i, all RPs under the BSS-i fail. The i-th BSS-W inrush occurs in the working face.

Application and Verification

The RP method was applied and BSS-W was identified at the Yuanzigou coal mine, which serves as a case study.

Project Background

The Yuanzigou coal mine, located in northwest Linyou county, Baoji city, Shanxi province, China, is part of the southern edge of the Longdong loess plateau (Fig. 1). The Guojiahe, Cuimu, and Xiaozhuang coal mines are all nearby and BSS-W inrush events have occurred in all of these coal mines. The stratigraphic sequence, from older to younger strata, follows: Triassic system Tongchuan formation(T_2t); Jurassic system: Fuxian formation (J_1f), Yanan formation (J_2y), Hiluo formation (J_2z), and Anding formation (J_2a); Cretaceous system: Yijun formation (K_1y), Luohe formation (K_1l), Huachi formation (K_1h), and Luohandong formation (K_1lh); Cenozoic Neogene, and quaternary. The coal seam thickness averages 10 m. Fully mechanized sublevel caving mining has disturbed and fractured the roof overburden. The K_1y conglomerate and the K_1l sandstone are aquifers. The borehole pumping test in the J_2z sandstone showed a unit inflow of 0.000046 ~ 0.0353 L/s·m of water; its permeability coefficient is 0.00038 ~ 0.0064 m/d.

Results and Discussions

The overburden of working face 1,012,001 was simplified as an RP model (Fig. 3) and divided into 24 RPs. The BSS distribution was calculated using the RP method after the working face had advanced by 200 m. Figure 4 shows how the rock mechanics parameters of the overburden were determined. Rock samples were taken from overburden cores and tested using a MTS 815.02 electro-hydraulic servo control rock mechanics testing system. Table 1 shows the mechanical parameters.

The BSS was identified according to RP theory (Fig. 5). The left side of Fig. 5 represents the scale of the thickness of the RP. Figure 5 shows the f value of RP-1 ~ RP-16. According to the RP instability criteria, if $f > 0$, it indicates that the RP is broken. As the working face advanced by 200 m, the first 12 RPs broke without significant amounts of BSS forming. Part of RP-13 broke, but it is a mudstone, with poor water penetrability, making it a favorable aquiclude. RP-14 is a sandstone, with $f < 0$, indicating that RP-14 is not broken. Therefore, the first BSS (BSS-1) formed between RP-13 and RP-14. The size of BSS-1 was calculated, and its shape was drawn based on RP theory.

Figure 7c shows the convex shape of BSS-1 with the maximum deformation in the middle of the RP. According to RP theory, BSS-1 has the largest volume, 8.9513 e4 m^3. Rock plates 15 through 23 were unbroken. As the working face advanced 200 m, the height of the fissure zone reached the location of RP-13, at 248 m. Since $W_{15} > W_{14}$, there was no BSS between RP-14 and RP-15; Since $W_{16} < W_{15}$, there

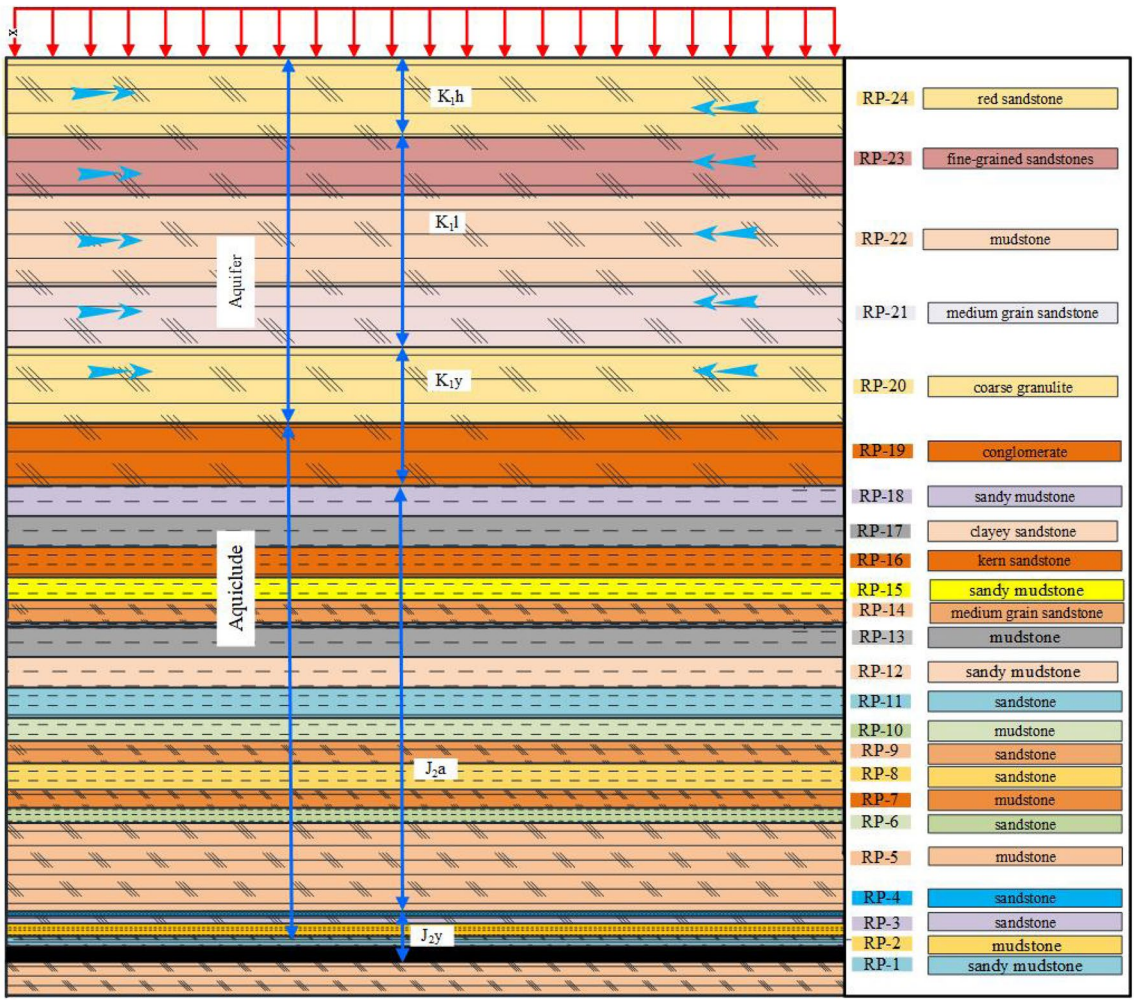

Fig. 3 RP model of the 1012001working face

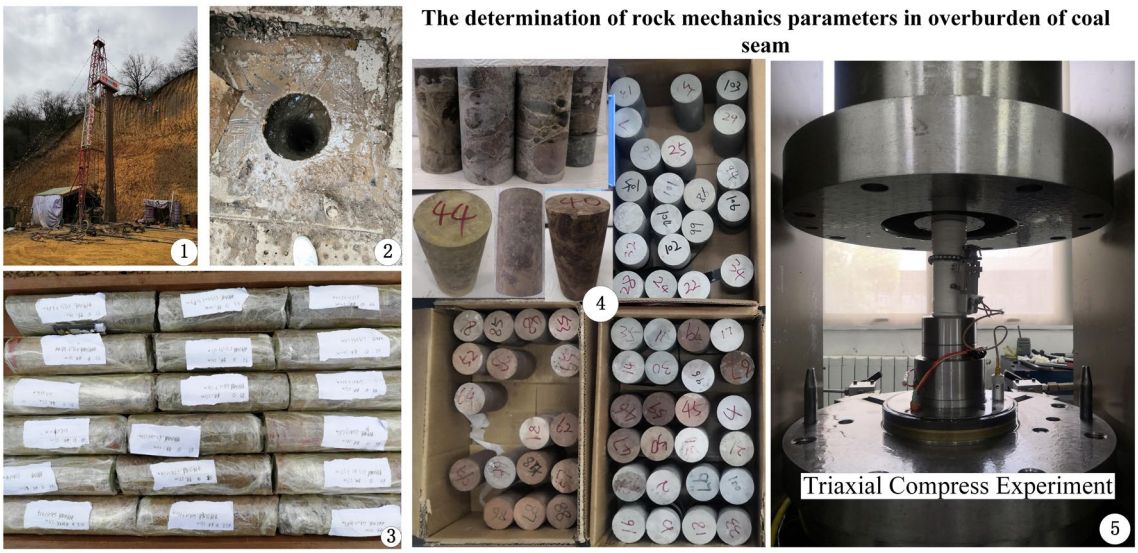

Fig. 4 The process of determining rock mechanics parameters in the overburden of the coal seam

Table 1 Physical and mechanical parameters of RPs

Num	Thickness (m)	Rock category	Density g/cm^3	E (10^4 MPa)	c (MPa)	p_o	φ (°)
24	14	Red sandstone	2.6	3.2	2.4	0.25	56
23	27	Fine-grained sandstones	2.5	3.8	2.1	0.24	50
22	8.5	Mudstone	2.0	2.1	0.21	0.45	28
21	8	Medium grain sandstone	2.6	3.4	1.7	0.21	58
20	19	Coarse granulite	2.1	2.6	1.5	0.4	34
19	14	Conglomerate	2.0	2.1	0.21	0.41	28
18	12	Sandy mudstone	2.1	2.6	1.5	0.35	34
17	20	Clayey sandstone	2.5	2.9	1.5	0.22	52
16	40	Kern sandstone	2.5	3.1	2.8	0.22	55
15	16	Sandy mudstone	2.1	2.4	1.7	0.3	40
14	20	Medium grain sandstone	2.6	3.5	2.4	0.24	56
13	20	Mudstone	2.1	2.6	1.5	0.36	34
12	30	Sandy mudstone	2.0	2.1	0.21	0.30	28
11	20	Sandstone	2.6	3.22	2.8	0.18	56
10	20	Mudstone	2.1	2.1	0.21	0.30	28
9	16	Sandstone	2.6	3.2	2.4	0.18	48
8	32	Sandstone	2.0	2.1	0.21	0.31	28
7	20	Mudstone	2.0	2.1	0.21	0.31	28
6	22	Sandstone	2.6	3.2	2.4	0.18	48
5	22	Mudstone	2.0	2.1	0.31	0.33	28
4	16	Sandstone	2.3	3.4	2.2	0.23	54
3	14	Sandstone	2.5	3.4	2.2	0.24	54
2	20	Mudstone	2.0	2.1	0.21	0.32	28
1	16	Sandy mudstone	2.1	1.2-	0.21	0.24	30

E elasticity modulus, *Po* Poisson ratio

was a second BSS (BSS-2) between RP-15 and RP-16, with a volume of 1.3466 e4 m^3. RP-16 is a hard sandstone and RP-15 is a soft mudstone, fulfilling the geological requirements of BSS; hard rock overlying soft rock. Considering that $W_{17} > W_{16}$, there was no BSS between RP-16 and RP-17. Since $W_{18} < W_{17}$, there was a third BSS (BSS-3) between RP-17 and RP-18, with a volume of 5.6574 e3 m^3. The upper RP of BSS is a conglomerate and the bottom RP of BSS is a mudstone. Considering that $W_{19} > W_{18}$, there is no BSS between RP-19 and RP-18. However, $W_{20} < W_{19}$, so there was a fourth BSS (BSS-4) between RP-20 and RP-19, with a volume of 638.0847 m^3. $W_{21} > W_{20}$, so there was no BSS between RP-21 and RP-20. Figure 6 shows the differences among W_{21}, W_{22}, and W_{23}, but these differences were small, allowing the BSS to be ignored.

Figure 7 shows the results. As the working face advanced 200 m, four BSSs were generated above the coal seam. BSS-1 was located at the contact surface between RP-14 and RP-13, 268 m above the coal seam. Since the upper rock of this BSS is not an aquifer, BSS-W was not generated. BSS-2 is located at the contact surface between RP-16 (fine-grained sandstone) and RP-15 (mudstone) 308 m above the coal seam. Again, since the upper rock of BSS-2 is not an aquifer, BSS-W was not generated. BSS-3 is located between the coarse granulite (RP-18) and mudstone (RP-17), 364 m above the coal seam. Since the upper strata of the BSS is an aquifer and the lower strata of BSS is an aquiclude, BSS-W did accumulate in BSS-3. BSS-4 was located between coarse granulite (RP-20) and mudstone (RP-19) 390 m above the coal seam. Again, since the upper strata, RP-20, is an aquifer, and RP-19 is an aquiclude, BSS-W accumulated in BSS-4.

Verification

The calculation results of the RP method were verified by borehole video observation. The field experiment mechanism is shown in Fig. 8. First, a hole (Φ150 mm) was drilled into the ground above the coal goaf. Observation equipment was installed when the amount of water in the hole was extremely small. The observation experiment was performed

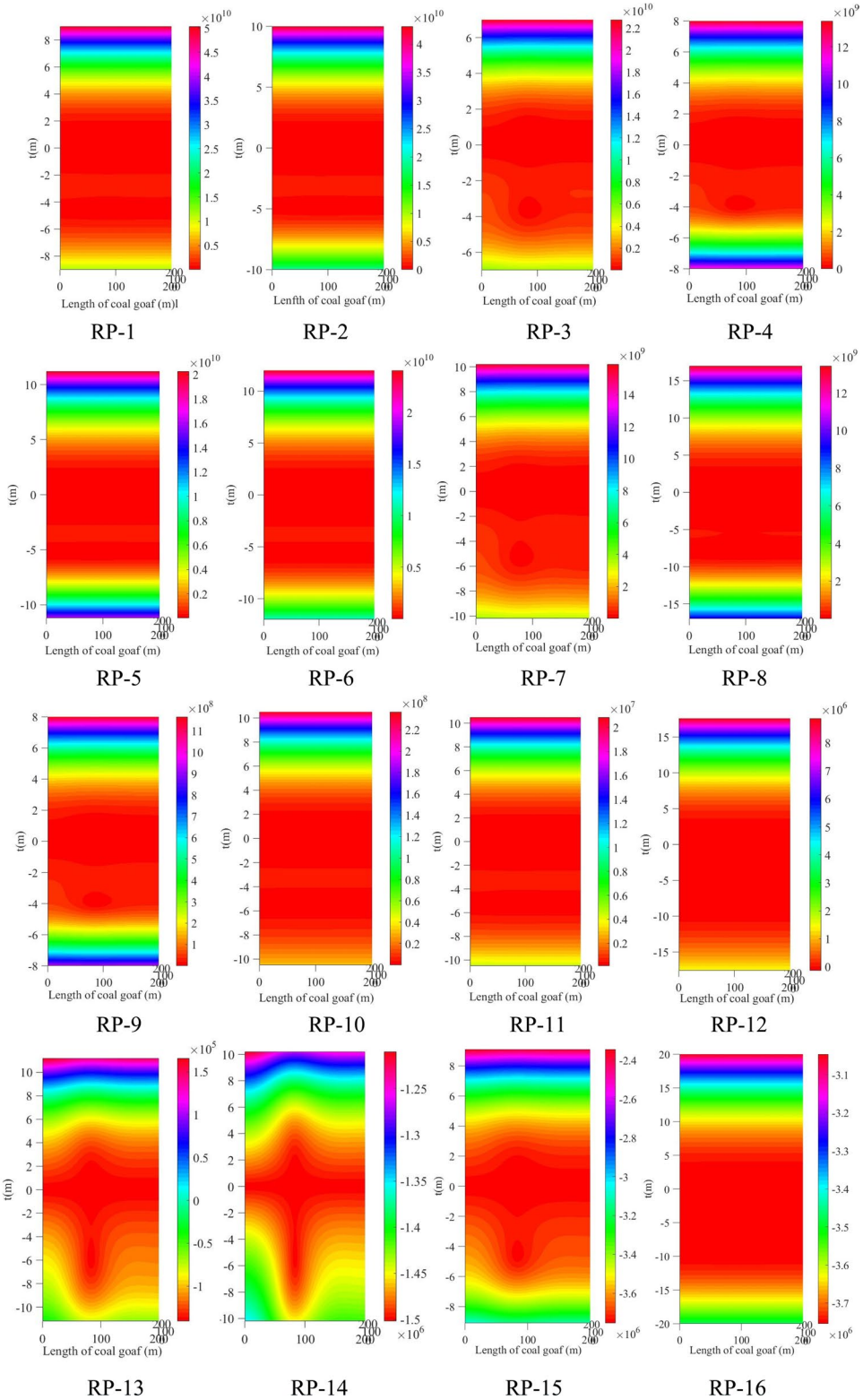

Fig. 5 The overburden state of the coal seam

with the camera moving at a very slow rate. Then, the results were analyzed in case it had to be redone.

The maximum height of the fissure zone and location of BSSs was determined by analyzing the distribution of the fractures and the BSS. Figure 9 shows the observed results. At a depth of 180 m below the ground, there was no fissure and the rock strata were unbroken. At a depth of 264 m, the stratum was fractured rock with Luohe formation water.

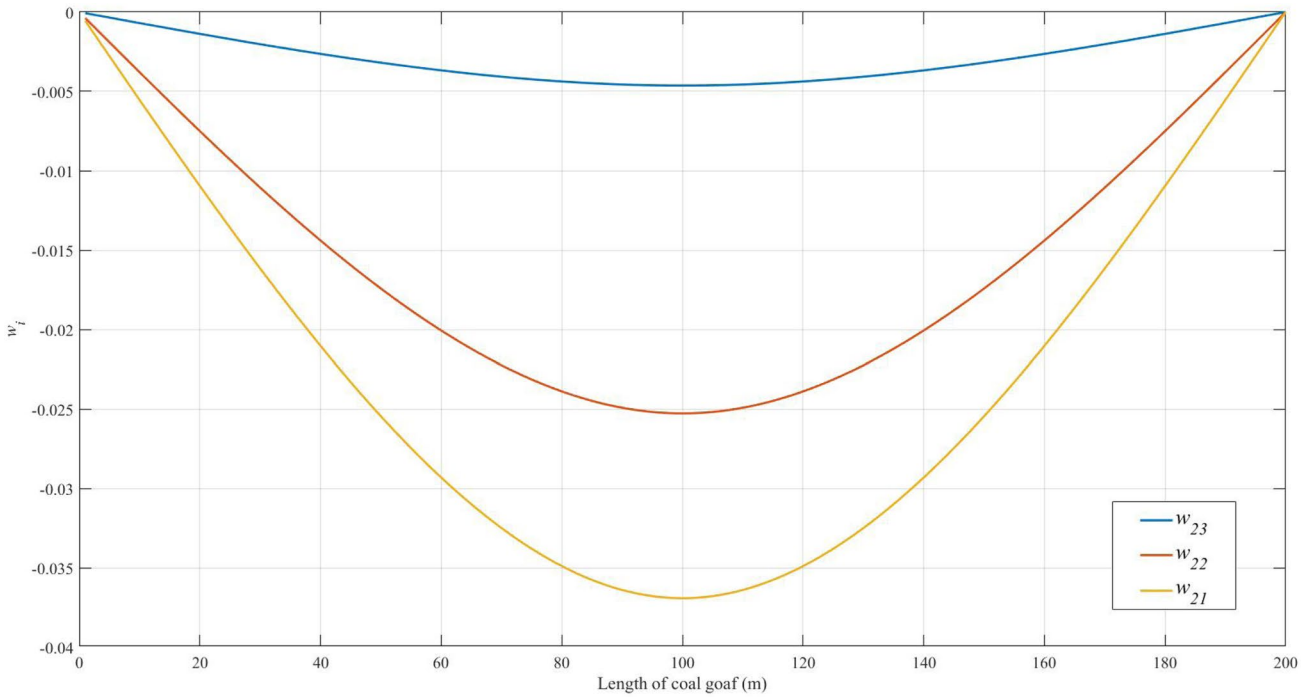

Fig. 6 The deflection value of RP-21 RP-22, and RP-23

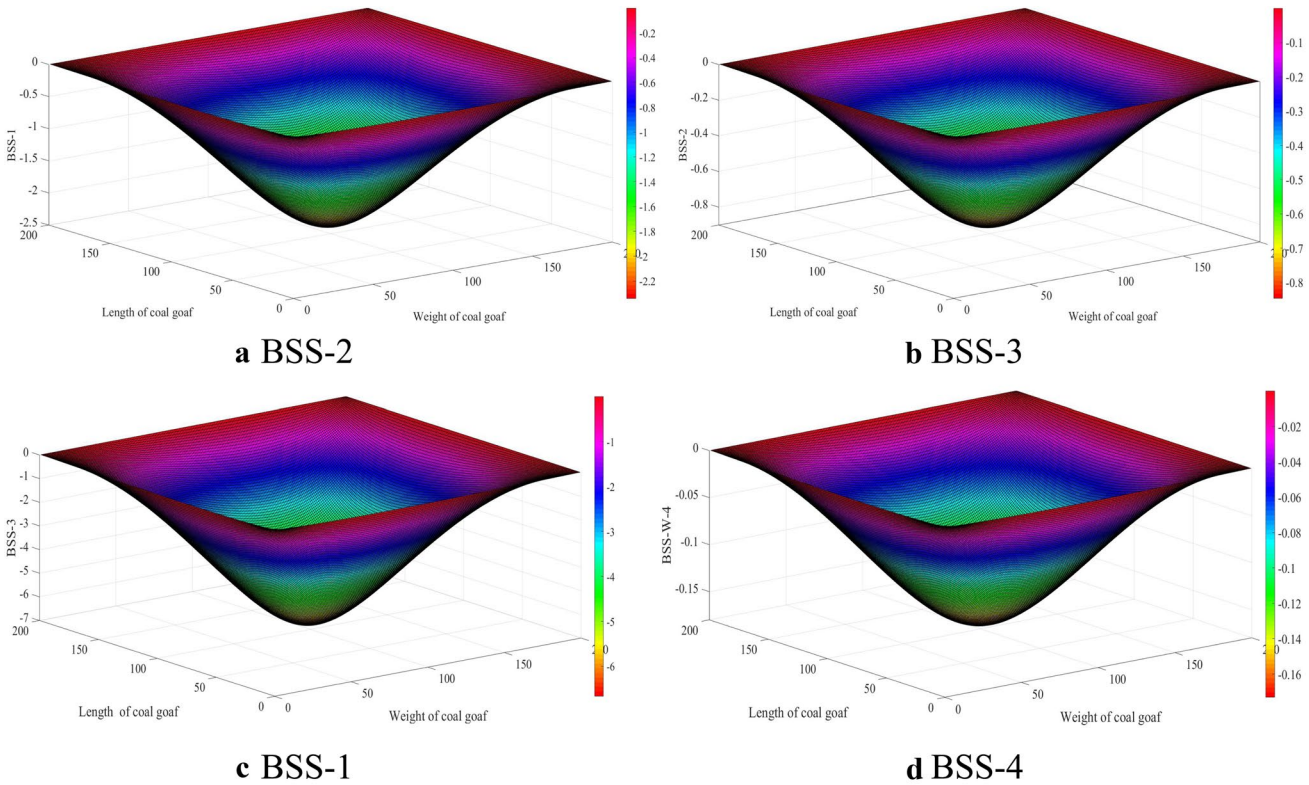

Fig. 7 The size of third BSS-W

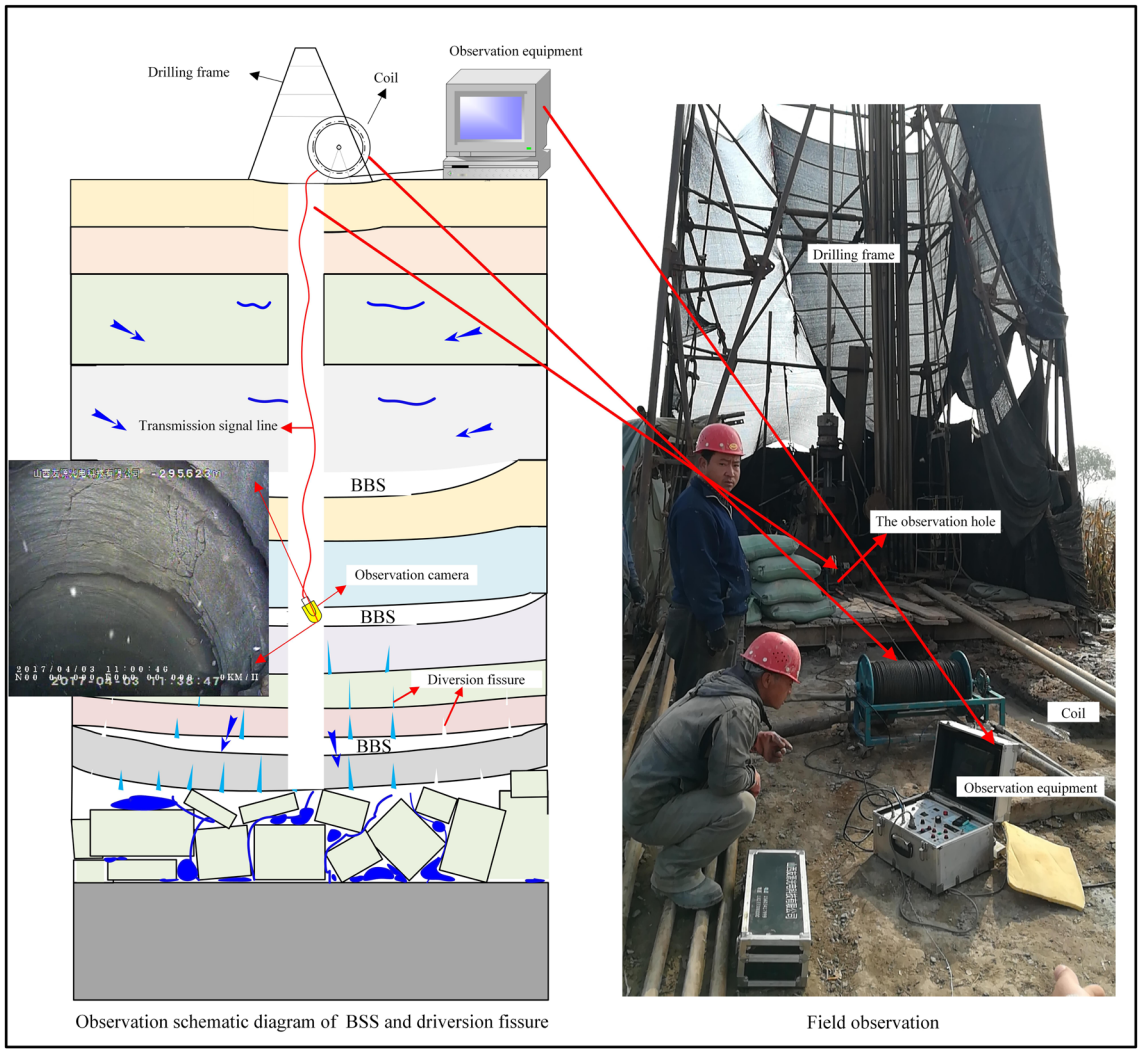

Fig. 8 Field observation experiment of BSS

When the depth was 298 m (390 m above the coal seam), there was BSS between RP-20 and RP-19, and BSS-W in the BSS, which is consistent with the RP method result. At a depth of 324 m (364 m above the coal seam, there was also BSS-W, in the BSS between the RP-18 and RP-17. At 420 m below ground, between RP-14 and RP-13, there was a BSS without BSS-W, which is also consistent with the RP results. When the depth was 452 m within RP-11, longitudinal fissures began to appear. BSS without water was also observed at 470 m, between RP-11 and RP-10. At 558 m, between RP-8 and RP-7, there was a longitudinal fissure along with a BSS, which had broken. A BSS penetrated by a longitudinal fissure was also observed at a depth of 600 m, between RP-6 and RP-5. Figure 10 shows the calculated and observed results.

The results are quite impressive, with the only significant exception being that no BSS was observed between RP-15 and RP-16. This could be due to the simplification of the computational model or because the characteristics of rock strata varied there. In future research, it is important to consider the heterogeneity and anisotropic nature of rock strata in the composite RP.

Assessment of BSS-W Inrush Disaster Risk

A small amount of BSS-W does not pose a threat to the personnel and equipment in the working face. However, as water accumulates in a BSS, a BSS-W inrush can occur in the working face very soon after a BSS fails, potentially causing casualties and equipment losses. According to the calculated results and analysis, the first BSS-W

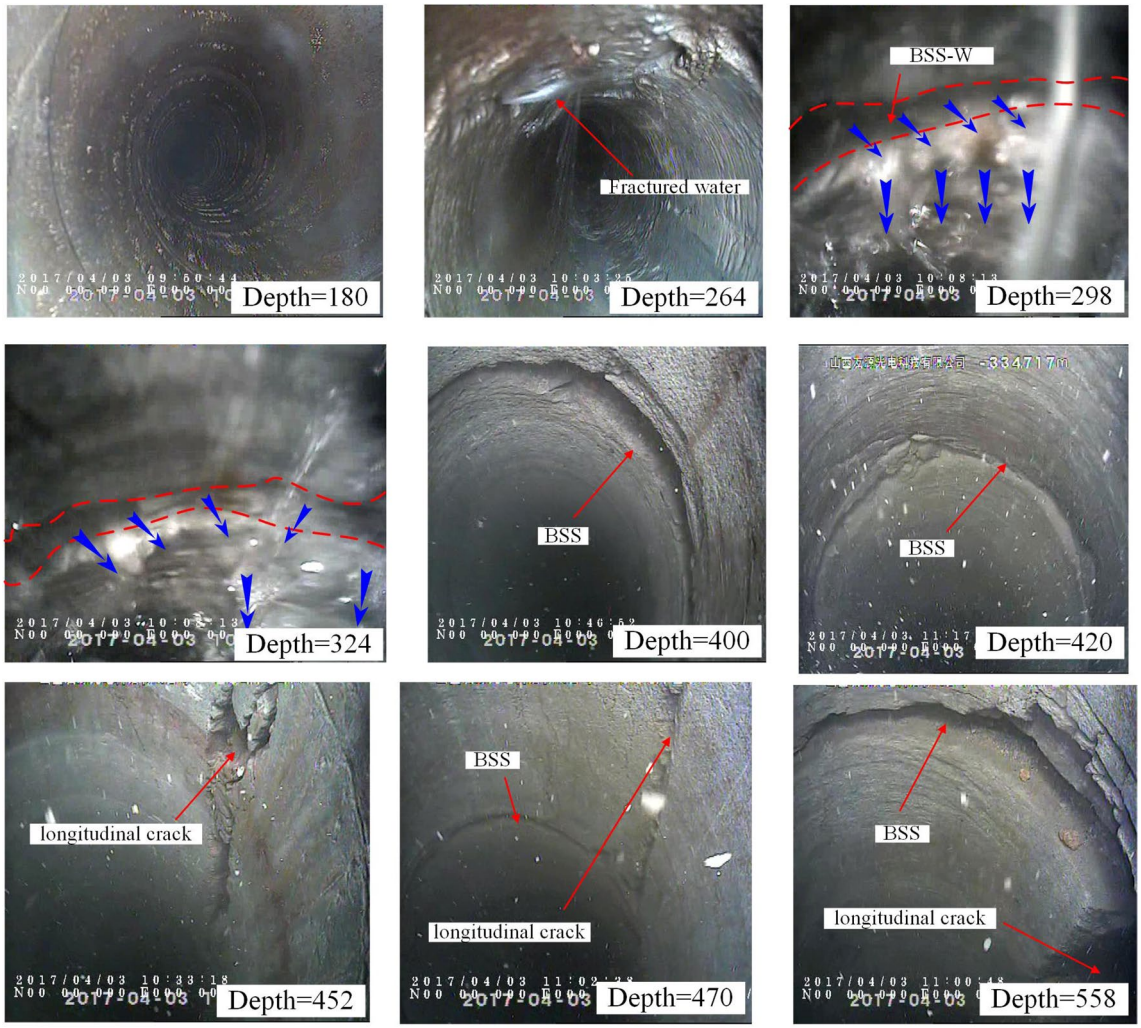

Fig. 9 Borehole video observation

was located between the conglomerate and mudstone in the Yijun formation and the second was between the conglomerate and medium-grained sandstone in the Luohe formation. The advance distance of the working face was calculated using the RP method, assuming that BSS-W-1 was broken. When the working face had advanced by 350 m, the RP-16 and RP-17 strata were in partial failure (Fig. 11a, b), but the integrity of BSS-W was still maintained. As shown in Fig. 11c, d, when the working face had advanced by 390 m, both RP-16 and RP-17 were broken, indicating that BSS-3 was broken, allowing BSS-W-1 inrush in the working face. At this point in time, the volume of BSS-W-1 was 5.6017 e4 m^3. Then, the volume of BSS-W was calculated, assuming a working face advance of 10 m/d; the volume of BSS-W-1 was calculated as 7.7619 e4 m^3. Although BSS-W-1 has a larger volume than BSS-3, the volume of BSS-W-1 equals the volume of BSS-3. Therefore, BSS-3 fills with water before BSS-3 is broken. It is obvious that the volume of BSS-W is large and can cause a water inrush disaster. Therefore, some measures had to be taken to prevent the hazard.

Next, the state of BSS-W-2 was analyzed as the working face advanced. Figure 12 shows the state of RP-19 when the working face had advanced by 400, 800, 1000, and 1120 m, respectively. RP-19 is stable, indicating that the BSS-4 was unbroken, and that BSS-W-2 would not cause a water inrush disaster.

BSS-W Inrush Prevention

Sufficient BSS and BSS-W are required for a BSS-W inrush disaster to occur. Therefore, certain measures should be taken to drain the BSS-W before the BSS fails. Here, we implemented two preventive measures: vertical drainage boreholes drilled from the ground above the working face

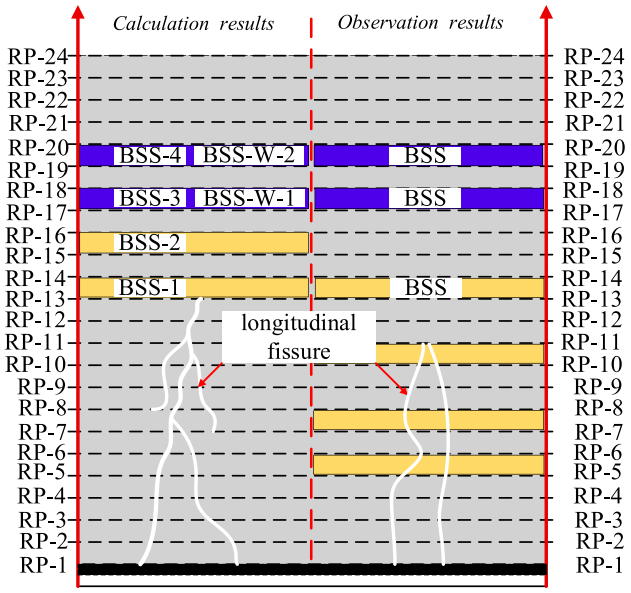

Fig. 10 Comparing and analyzing observations and calculations results

and inclined drainage boreholes drilled from the roadway to discharge the BSS-W before an inrush could occur.

Inclined drainage holes in the roadway were used to drain and discharge water stored in the sandstone fissure and the BSS-W, so that the water could not continue to accumulate in the BSS. When designing the azimuth, inclination angle, number, and length of the drainage holes, the location of the aquifer and construction conditions had to be considered, including the power of the drilling rig and the experience of the workers. Figures 13 shows the design scheme, the discharge of the BSS-W and fissure water, and the drilling performed on site.

The maximum height of the inclined drainage pipe in the roadway was limited because of inadequate drilling rig power and complex construction conditions. When the location of the BSS-W was beyond the maximum height of the inclined drainage pipe, the upper BSS-W that could not be discharged by the inclined drain in a timely manner. Therefore, a vertical drainage hole was drilled from the surface to discharge the BSS-W in advance (Fig. 14). The required using RP theory to determine the height of the fracture zone and identify the location of the BSS-W.

To discharge the BSS-W in advance, the borehole should connect to the fracture zone and H_b should conform to Eq. (6). To reduce the drainage, a drive pipe was used to stop up the aquifer, to prevent the water from flowing into the working face through the drainage hole and fracture zone. Therefore, H_d should conform to Eq. (7).

$$H_b \geq H_{tot} - H_{frac}, \tag{6}$$

$$H_d = h_{BSS-3} + 2. \tag{7}$$

After the drainage hole was drilled, we installed the drive pipe and monitored the water level in the borehole; pumping was adjusted any time the water level suddenly dropped. Additional holes were drilled to drain areas with abundant water. The design and construction of a drainage hole are shown in Fig. 14.

Conclusions

In coal mining, BSS-W inrushes can cause casualties and economic losses. To avoid such a disaster, the RP method was used to determine the location and size of the BSS-W. This method was verified by borehole video observation. The RP method involves: treating the upper overburden of the coal seam as a combined rock plate based on rock strata classification; assuming that the shape of the RPs is the same

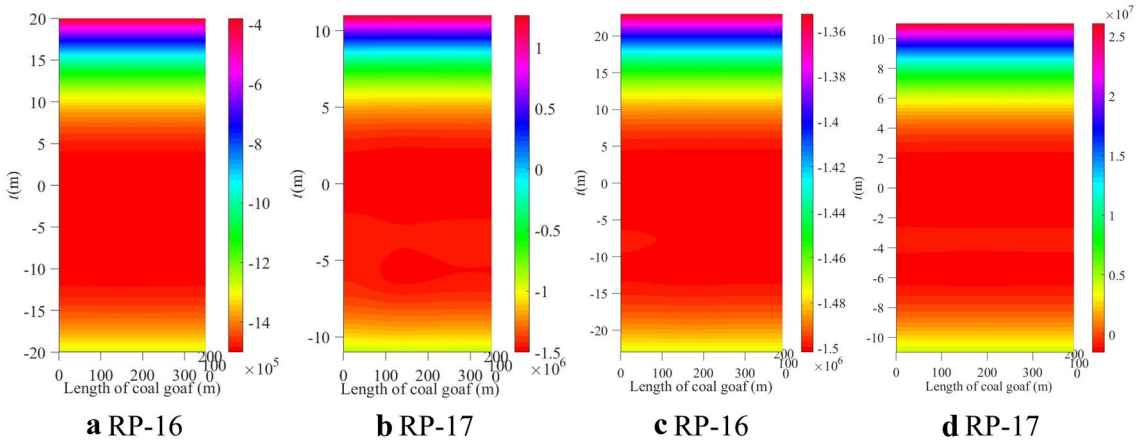

Fig. 11 The state of RP-16 and RP-17

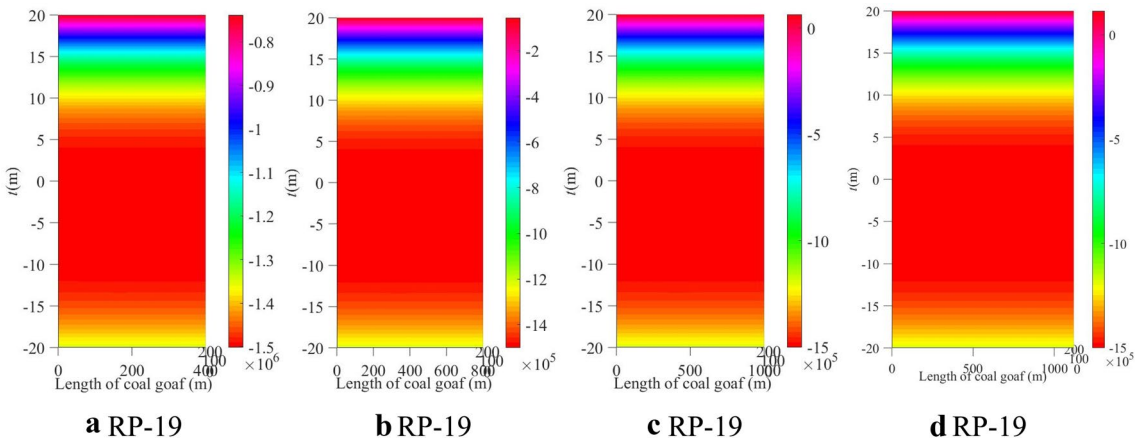

Fig. 12 The state of RP-19 as the length of coal goaf extends 400, 800, 1000, and 1120 m

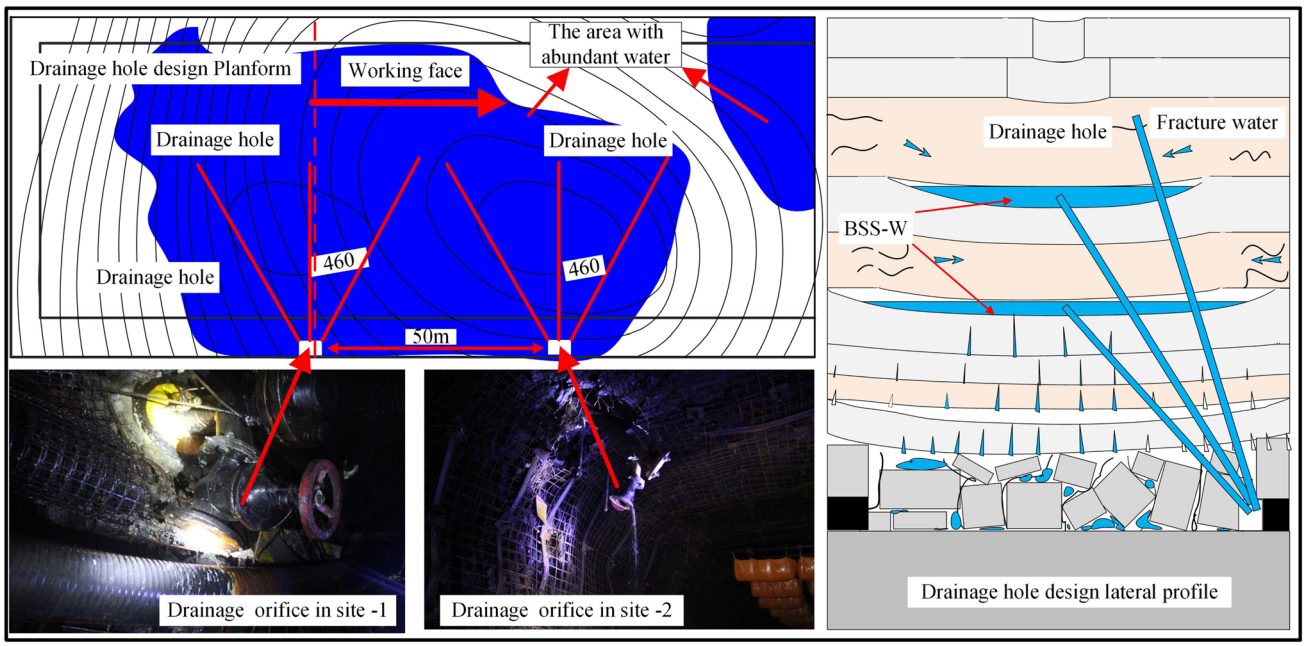

Fig. 13 Inclined drain hole design

as that of the coal goaf, and where appropriate, rectangular; calculating an analytical solution of the RP through a double trigonometric series of deflections of the *w* of RP. The deflection function *w* (x, y) is deduced by the reciprocal work theorem, which allows the internal forces of RP to be expressed by *w* (x, y). Then the internal forces and deformation of the RP plate are calculated based on the weight (x) and length (y) of coal goaf. Finally, the size and location of the BSS-W are determined using the proposed BSS identification method.

The RP method was verified in the Yuanzigou coal mine. The calculated results indicated that two BSS-W would form above the coal seam as the working face advanced 200 m. The first predicted BSS-W was located 364 m above the coal seam, between RP-18 and RP-17 and was 5.6017 e4 m^3 in size, which is dangerous. A second BSS-W was located between RP-20 and RP-19. Therefore, it was necessary to assess this risk and take measures to prevent a BSS-W inrush.

The height of the fissure zone and the location of the BSS was confirmed by borehole video observation. The observed results were virtually the same as the calculated results and

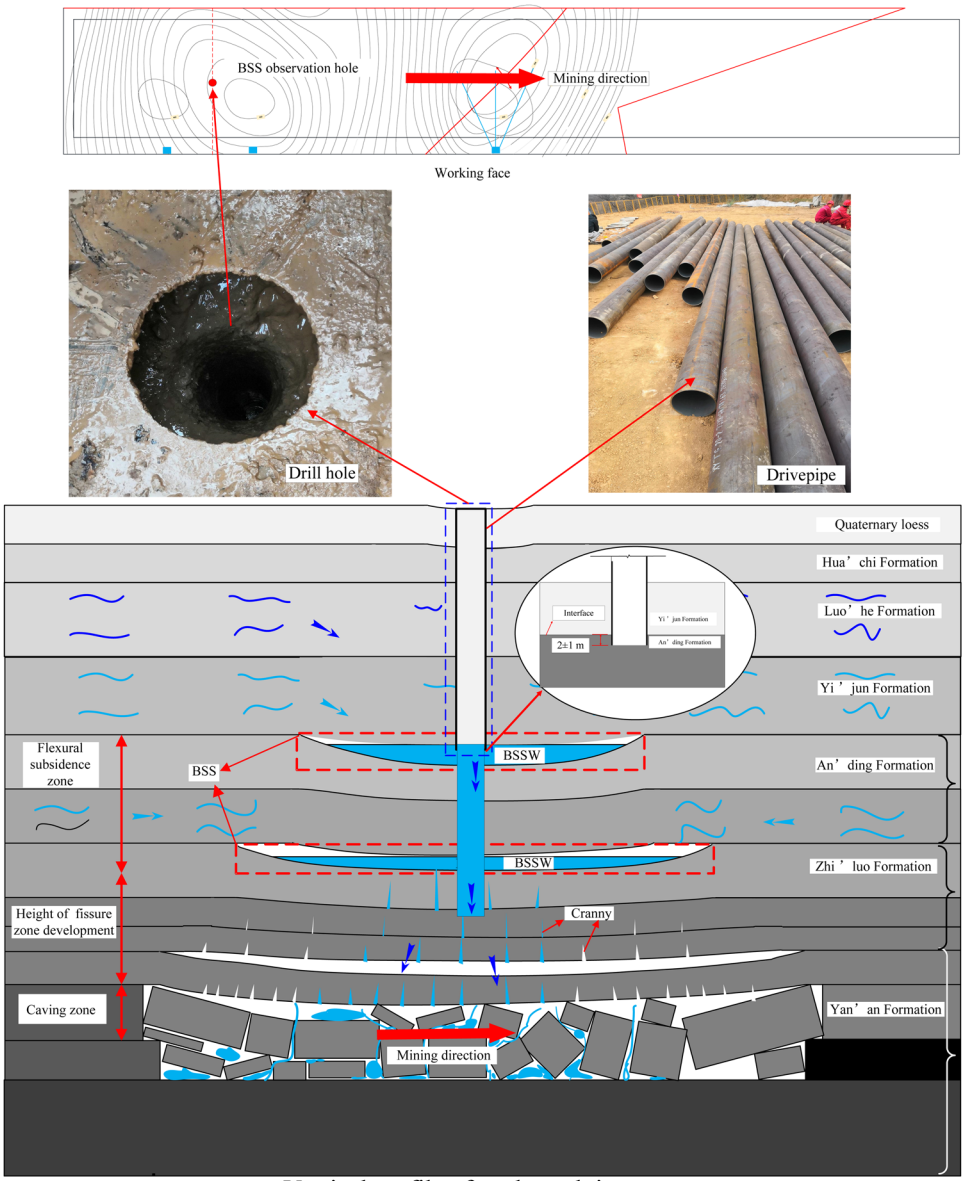

Vertical profile of coal overlying strata

Fig. 14 Vertical drain hole design drilled from above

confirmed that large BSS usually occurs between hard and soft rock strata.

Then, two BSS-W inrush control methods were investigated. The first involved constructing inclined drainage holes in the roadway to drain and discharge the water stored in the sandstone fissure and BSS-W. However, the length of inclined drainage holes in the roadway was limited because of construction conditions; only the lower BSS-W could be drained in advance in this manner. Therefore, holes were also drilled from the surface into areas with abundant water. This allowed BSS-W and water in the fissured zone to be discharged before the working face came too close to the hazards. This was successfully implemented, and no BSS-WIH happened in working face 1,012,001 in the Yuanzi Gou coal mine.

The RP method has certain limitations and disadvantages: (1) there may be some errors in calculation, since thickness inconsistencies and complex geological conditions, such as faults, synclines, and anticlines are ignored. (2) The calculated volume of BSS-W is actually larger than the real volume, since water seepage is assumed to conform to Darcy's law, and A is always equal to a × b. (3) In practical geological conditions, the lateral stress coefficient is complex and influenced by many factors. Therefore, the value of the lateral stress coefficient in the paper is not precise.

Acknowledgements This work was supported by the National Natural Science Foundation of China (41977238 and 51804339), the Young Elite Scientists Sponsorship by CAST, the Special Fund for the Construction of Innovative Provinces in Hunan (2019RS2007), and the China Postdoctoral Science Foundation (2019T120715 and 2018M640760).

References

Cao HD (2018) Study on prevention & control technology and disaster-caused mechanism of bed separation water body in overburden strata during coal seam mining. PhD thesis, China Coal Research Institute, Beijing **(in Chinese)**

Chen SG, Guo H (2008) Numerical simulation of bed separation development and grout injecting into separations. Geotech Geol Eng 26(4):375–385. https://doi.org/10.1007/s10706-008-9174-7

Fan KF, Li WP, Wang QQ, Liu SL, Xue S, Xie CY (2019) Formation mechanism and prediction method of water inrush from separated stratas with in coal seam mining: a case study in the Shilawusu mining area. China Eng Fail Anal 103:158–172. https://doi.org/10.1016/j.engfailanal.2019.04.057

Gao F, Sang Y (2017) Water inrush from overburden strata separation reservoir and the countermeasures in Lijialou coal mine. J N Chin Inst Sci Technol 14(6):12–16 (**in Chinese**)

Gui HR, Lin ML, Song XM (2018) Identification and application or roof bed separation (water) in coal mines. Mine Water Environ 37(2):376–384. https://doi.org/10.1007/s10230-018-0518-0

Guo WJ, Li YY, Yin DW, Zhang SC, Sun X (2016) Mechanisms of rock burst in hard and thick upper strata and rock-burst controlling technology. Arab J Geosci 9(10):1–11. https://doi.org/10.1007/s12517-016-2596-2

He JH (2018) Dynamic evolution of bed separation in coal seam mining and assessment of bed-separation water hazards. PhD He, China Univ of Mining and Technology **(in Chinese)**

He JH, Li WP, Liu Y, Yang Z, Liu SL, Li LF (2018) An improved method for determining the position of overlying separated strata in mining. Eng Fail Anal 83:17–29. https://doi.org/10.1016/j.engfailanal.2017.09.015cc

Li XQ (2011) Study on the inrush mechanism of the water in bed separation due to repeated coal mining under hard rock. PhD Li, China Univ of Mining and Technology **(in Chinese)**

Lin Q, Qiao W (2016) Water prevention and control technology of roof bed separation in Cuimu Mine. Coal Sci Technol 44(3):129–134 (**in Chinese**)

Lu QY, Li XQ, Li WP, Chen W, Li L, Liu S (2018) Risk evaluation of bed separation water inrush: a case study in the Yangliu coal mine. China Mine Water Environ 37(2):288–299. https://doi.org/10.1007/s10230-018-0535-z

Ma D, Duan H, Li X, Li Z, Zhou Z, Li T (2019) Effects of seepage-induced erosion on nonlinear hydraulic properties of broken red sandstones. Tunn Undergr Sp Tech. https://doi.org/10.1016/j.tust.2019.102993

Ma D, Duan H, Liu W, Ma X, Tao M (2020a) Water–sediment two-phase flow inrush hazard in rock fractures of overburden strata during coal mining. Mine Water Environ 39(2):308–319. https://doi.org/10.1007/s10230-020-00687-6

Ma D, Duan H, Zhang Q, Zhang J, Li W, Zhou Z, Liu W (2020b) A numerical gas fracturing model of coupled thermal, flowing and mechanical effects. Comput Mater Cont 65(3):2123–2141. https://doi.org/10.32604/cmc.2020.011430

Ma D, Zhang J, Duan H, Huang Y, Li M, Sun Q, Zhou N (2021) Reutilization of gangue wastes in underground backfilling mining: Overburden aquifer protection. Chemosphere 264:128400

Miao X, Cui X, Wang J, Xu J (2011) The height of fractured water conducting zone in undermined rock strata. Eng Geol 120(1–4):32–39. https://doi.org/10.1016/j.enggeo.2011.03.009

Palchik V (2003) Formation of fractured zones in overburden due to long wall mining. Environ Geol 44(1):28–38. https://doi.org/10.1007/s00254-002-0732-7

Palchik V (2005) Localization of mining-induced horizontal fractures along rock strata interfaces in overburden: field measurements and prediction. Eng Geol 48(1):68–80. https://doi.org/10.1007/s00254-005-1261-y

Qian MG, Miao XX, Xu JL (2003) Key strata theory in ground control. China Univ of Mining and Technology press, Xuzhou (**in Chinese**)

Qiao W, Li WP, Li XQ (2011) Mechanism of "hydrostatic water inrush" and counter measures for water inrush in roof bed separation of a mining face. J Min Saf Eng 28(1):96–104 (**in Chinese**)

Qiao W, Huang Y, Yuan ZB, Guo W, Zhou DK (2014) Formation and prevention of water inrush from roof bed separation with full-mechanized caving mining of ultra-thick coal seam. Chin J Rock Mech Eng 33(10):2076–2084 (**in Chinese**)

Su ZJ, Yu GM, Yang L (2003) Numerical simulation on mechanism of deformation of separated strata in overburden. Chin J Rock Mech Eng 22(8):1287–1290 (**in Chinese**)

Wang SF, Li XB, Wang SY (2017) Separation and fracturing in overlying strata disturbed by long wall mining in a mineral deposit seam. Eng Geol 226:257–266. https://doi.org/10.1016/j.enggeo.2017.06.015

Wu LY, Bai HB, Yuan C, Wu GM, Xu CY, Du Y (2019) A water-rock coupled model for fault water inrush: a case study in Xiaochang coal mine, China. Adv Civ Eng 2019:1–12. https://doi.org/10.1155/2019/9343917

Xu JL, Qian MG, Jin HW (2004) Study and application of bed separation distribution and development in the process of strata movement. Chin J Geotech Eng 26(5):632–636 (**in Chinese**)

Xu JL, Wang XZ, Liu WT, Wang ZG (2009) Effects of primary key stratum location on height of water flowing fracture zone. Chin J Rock Mech Eng 28(2):380–385 (**in Chinese**)

Xuan DY, Xu JL (2014) Grout injection into bed separation to control surface subsidence during longwall mining under villages: case study of Liudian coal mine. China Nat Hazards 73(2):883–906. https://doi.org/10.1007/s11069-014-1113-8

Yan H, He FL, Yang T, Li LY, Zhang SB, Zhang JX (2016) The mechanism of bedding separation in roof strata overlying a roadway within a thick coal seam: a case study the Pingshuo coalfield, China. Eng Fail Anal 62:75–92. https://doi.org/10.1016/j.engfailanal.2015.12.006

Zhou ZL, Cai X, Ma D, Chen L, Wang SF, Tan LH (2018) Dynamic tensile properties of sandstone subjected to wetting and drying cycles. Constr Build Mater 182:215–232. https://doi.org/10.1016/j.conbuildmat.2018.06.056